

Effect of mass ratio of titanium dioxide and oil palm fiber ash (TiO₂: Ash) in hybrid photocatalyst on photocatalytic seawater pretreatment

Abdulkarim Suliman, Ruzinah Isha, Jamil Roslan
Faculty of Chemical and Natural Resources Engineering
University Malaysia Pahang
Lebuhraya Tun Razak, 23600 Kuantan Pahang, Malaysia
kaarim1980@gmail.com, ruzinah@ump.edu.my

Abstract— Titanium dioxide (TiO₂) has been used in a wide variety of applications such as air purification, water purification and photo electrochemical conversion systems. However, the development of advanced materials with enhanced performance for catalytic applications especially in water treatment is highly required. The objective of this work is to study the effect of hybrid titanium dioxide (TiO₂) photocatalyst in pretreatment seawater desalination. The catalyst with mass ratio of TiO₂: palm oil fiber ash (POFA) at 0:100, 40:60, 60:40 and 100:0 was synthesized via wet impregnation. The catalyst was calcined at 500 °C for four hours. The mixture of artificial seawater and catalyst at mass ratio of photocatalyst: artificial seawater at 1:300 was put in a one-liter borosilicate photo-reactor that fixed with mercury light of 350 nm for two hours with stirring at 1000 rpm. The pH, total dissolved solid (TDS), conductivity (EC), turbidity and chemical oxygen demand (COD) of the artificial seawater was analyzed before and after the investigation. The fresh and spent catalysts were characterized via X-Ray Diffractogram (XRD), Nitrogen physisorption analysis, Scanning Electron Microscopy (SEM) and Energy Dispersive X-Ray Spectroscopy (EDX). It is found that the combination of TiO₂ and OPFA has dual function material, i.e. as photocatalyst to decompose the organic matter and as adsorbent to adsorb the salt in its pore. The catalyst with TiO₂: palm oil fiber ash (POFA) at 40:60 and 60:40 can reduce the COD at 45 % and 41% respectively. As more OPFA was added into the hybrid TiO₂ catalyst, the pH of the artificial seawater increased. It can be deduced that the hybrid TiO₂ photocatalyst that synthesized with OPFA has huge potential to treat seawater.

Keywords— desalination, Palm oil fiber ash, photocatalyst, seawater, Titanium dioxide

1. INTRODUCTION

Although the water covers the 75% of earth's surface, but the major portion of this water is covered by highly saline sea-water [1]. Due to the scarcity of fresh drinkable water, the desalination of sea-water sources has emerged as a prominent approach to meet the demand of clean potable water [2]. However, techniques for desalination require a high amount operational energy to convert the seawater to drinking water such as membrane and thermal desalination processes [3]. In addition, blocking of pore membranes and pipeline due to the deposition of the suspended solids during desalination process are the two critical problems, which increases the heat transfer coefficient and fuel consumption. Furthermore, these techniques also released large amount of greenhouse gases during processing [4]. Many research efforts have been devoted for water desalination to reduce the energy consumption [5]. The desalination with the photocatalytic method using semiconductor materials has been regarded as the promising approach. Moreover, this technique can also degrade the suspended solids and contaminants in the sea-water [6].

Semiconductor materials can enhance photocatalytic chemical reactions by facilitating the photogenerated electrons and holes by absorbing energy from sunlight and UV-light sources [7]. In addition, these materials have properties such as low cost, non-toxic, resistance toward photo-corrosion, and ability to absorb visible or near UV light [8]. Particularly, Titanium dioxide

(TiO₂), also known as Titanium (IV) oxide has been widely investigated for photolytic reactions in research and even at commercial sectors [9]. Moreover, TiO₂ was also used in many other applications such as electro-ceramic, glass and in photocatalytic degradation chemicals [10]. In photocatalytic desalination techniques, the catalytic activity of the TiO₂ can be improved by combining it with high surface area supported materials. Moreover, the light sources with different wavelength can be used for further improvements in this process [11]. Various advanced materials such as Zeolite, carbon nanotube and active carbon with porous structure were combined with TiO₂ to improve its dispersion in the photocatalyst [12] [13]. In this regard, the palm oil fiber ash (POFA) generated from palm oil mill have recently attracted research interest from different Malaysian research institutions. Since, oil palm plantation covers 5.1 million hectares of cultivated area and oil production of 18.8 million tones in Malaysia [14]. Besides, large amount of solid waste such as palm oil fiber ash (POFA), oil palm trunks (OPT), oil palm fronds (OPF), and empty fruit bunches (EFB) and palm pressed fibres (PPF), palm shells and palm oil mill effluent palm (POME) has been generating in the palm oil industries [15]. OPFA is a one of major non-toxic waste source and generally producing from the-product thermal power generation plants [16] [17]. POFA has also been used as adsorbent for wastewater treatment processes It was expected that the TiO₂ and POFA mixtures can be efficient to reduce the salinity of the sea-water and it could also remove the various contaminants by absorbing it on the surface [18]. Supported photocatalysts have good pollutant adsorption properties, diffusion properties, and high photocatalytic activities [19]. Therefore, this study has investigated a series of different TiO₂ and ash hybrid mixtures as photocatalysts to reduce the salt concentration in seawater by using the light wavelength of 365 nm.

2. METHODOLOGY

A. Materials

Palm oil fiber ash waste was procured from Felda Lepar Hilir 3 palm oil mill, Gambang, Kuantan, Pahang. It was obtained through the combustion of oil palm fiber in boiler to generate energy. The artificial seawater (ASW) was prepared by dissolving the 1 g of Humic acid in 1 L of deionized water, followed by addition of 2 to 3 pellets of NaOH to prepare a stock solution. Then adding 15 ml of stock solution to 1L of deionized water with 30 g of NaCL. The solution was mixing well with a stirrer to ensure that all salts are dissolved.

B. Catalyst preparation

Wetness Impregnation (WI) techniques was applied to synthesize all the photocatalysts. A series of photocatalysts using different percentage of weight ratios of TiO₂ to POFA (40:60 and 60:40) were used. In this technique, TiO₂ and POFA were mixed in deionized water and stirred at 80 °C for 4 h time span, followed by drying overnight at 100 °C in the oven. Finally, the as-obtained material was calcined at 500 °C in the furnace for 4 h. The catalyst was crushed and sieved to the size of < 125 μm to homogenize the size of catalyst

C. Catalyst characterization

Crystalline phases of all the fresh and spent photocatalysts were detected by using the X-ray powder diffraction (XRD) equipped with Cu K α source with a wavelength (λ) of 1.5405 Å at 15 mA and 30 kV and scanning in the 2 θ range of 10°-80° at 4° min⁻¹ via Rigaku Miniflex II. The BET surface area (m² g⁻¹), pore size (nm) and total pore volume (cm³ g⁻¹) of each catalyst were obtained via N₂ adsorption-desorption using Micro-meritics. Prior to the analysis, the catalyst was outgassed at 200°C for 6 h. Surface morphology tested by Scanning Electron Microscopy (SEM). Meanwhile, elements analysis identified by Energy Dispersive X-Ray Spectroscopy (EDX), by QUANTA 450 at the central laboratory, UMP.

D. Photocatalytic reactor setup

Briefly, 1 L borosilicate reactor was used to conduct the photocatalytic reaction on artificial seawater in the presence of UV light irradiation as shown in Fig. 1. The reactor was covered with aluminum foil to enhance the light intensity and reduce the energy loss from the photoreactor system during the reaction. Moreover, the reactor was coated with black color to prevent the interference of external light during the reaction. The reactor was equipped with the UV lamp with wavelength of 365 nm. Each run was performed for 2 h and simultaneously stirred at 400 rpm to ensure the complete mixing of the solution. In addition, the ratio of catalyst to seawater sample was. 1:300 in the final solution. Thus, about 2.7 g of the sample was added to the 800ml of artificial seawater (ASW). After the completion of the experiment, the catalyst was filtered out from all samples. Then, the catalyst was again characterized by various techniques such as EC, COD, PH and Turbidity of the water. Hach Sension+ 150 mm instrument was used to determine pH, conductivity (EC), and total dissolved solid (TDS) of the seawater. The COD

digestion Reagent Vial High Range using 435 COD HR instrument was conducted for both fresh and used catalyst to determine the organic compound in the artificial seawater. Meanwhile, the turbidity (ASW) was measured by Turbidity meter Hach 2100 model. All the measurements was repeated thrice for the reliability of the data and the average value was finally selected for this work. In this investigation, a pyramid cover for condensing and collecting freshwater was used instead of a vacuum pump and condenser to collect the distilled freshwater. This modification consists of two parts which are the pyramid roof with 45° for each side and square base with dimensions 18cm × 18cm. The square part is open from the bottom by opening a circular has the same inner diameter of the reactor which is 10.12 cm. The weight of these two parts 1.16 kg, so to know the amount of fresh water produced by the difference in pyramid weight before and after each experiment.

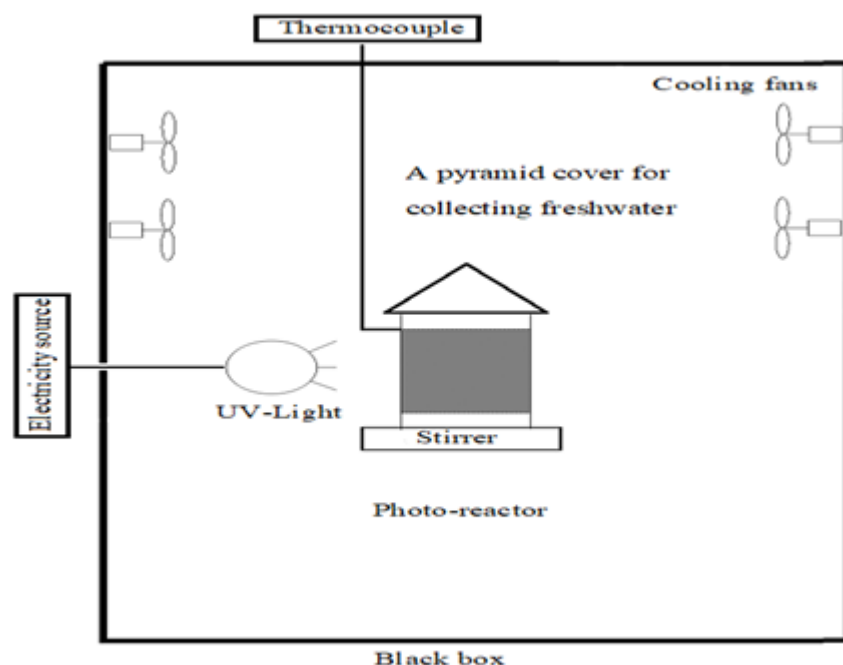


Figure 1: Schematic diagram of batch photocatalytic reactor set up

3. RESULTS AND DISCUSSION

A. Catalyst characterization

Table 1 summarized the BET surface area, pore volume and pore size of fresh and used photocatalysts of TiO₂, Ash and different Ti:Ash mixtures. The pore diameter in the range of 5.30 nm to 34.21 nm clearly indicated that all fresh and used photocatalysts exhibits mesoporous nature of materials. Surprisingly, BET surface area of Ti:Ash (ratio 100 to 0) or 100% TiO₂ was increased from 5.7 m²/g to 10.1 m²/g after the reaction. This could be due to the inflation character of TiO₂ in the water, which leads to increase in surface area of the catalyst after reaction [5]. However, the pore volume of Ti:Ash 100:0 was decreased from 5.6 × 10⁻² cm³/g to 4.2 × 10⁻² cm³/g, respectively. On the other hand, the specific surface area and pore volume of Ti:Ash 0:100 decreased after testing from 18.1 m²/g to 12.9 m²/g and 2 × 10⁻² cm³/g to 1.98 × 10⁻² cm³/g respectively, as well as the pore size also decreased from 7.12 nm to 5.3 nm. This was possibly due to the shrinkage of the structure of POFA by interacting with sea water. As shown in Table 1, the BET surface area, total pore volume and diameter for the TiO₂ and Ash mixture photocatalysts at different ratios (40:60 and 60:40) was increased after the reaction. This increasing trend again showed the predominance of TiO₂ in the catalyst mixture, which gets inflated after interacting with the water and increased the surface area of the overall catalysts. It was expected that the high values for pore size and BET surface area obtained for the TiO₂ and ash mixtures could increase the photo catalytic activity of the catalyst [20]. In addition, Guo *et al.* reported that smaller pore size was not compatible for the diffusion of the photoelectrons, which leads to decrease in the performance [21]. Moreover, Katou *et al.* and Grosso *et al.* showed that the open mesoporous structure was more efficient for the photocatalytic decomposition of dye, acetone, water [22, 23].

Table 1: Physical properties of TiO₂, Ash and Ti:Ash hybrid photocatalysts.

Catalyst weight ratio of TiO ₂ :Ash (%)	Specific surface area (m ² /g)		Pore volume ×10 ⁻² (cm ³ /g)		Pore size (nm)	
	Before	After	Before	After	Before	After
100% TiO ₂	5.7	10.1	5.6	4.2	22.2	23.2
100% Ash	18.1	12.9	2	0.3	7.1	5.3
40:60	3.9	6.1	1.7	3.2	21.5	17.4
60:40	4.3	11.0	3.6	4.9	34.2	18.1

Fig. 2 illustrates the fresh and spent XRD pattern of TiO₂ and palm oil fiber ash (OPFA) before and after testing in the photocatalytic reactor system. As seen in Fig. 2(a) and (b), the sharp peak and high intensity peak was observed for both fresh and spent catalysts at 2θ of 25.728° for pure ash (100% ash), indicating the crystalline nature of silicon oxide or silica. In addition, the anatase phase at 2θ of 27.081° was detected in 100% TiO₂ photocatalysts. Sun et al. reported that the different phases of TiO₂ can be obtained by varying the calcination temperature during its synthesis [24]. Therefore, the calcination temperature of 500 °C transformed rutile phase to anatase in this work. However, the transformation of anatase and brookite into rutile does not occur at the room temperature but both metastable phases become rutile when expose to high heat above 700 °C [25]. It was also reported that the impurities in the material can lead to transformation of anatase phase in the range of 600°C to 1100 °C temperatures [26]. It was reported that calcination temperature of 600°C was suitable for removing the impurities from the sample, moreover peak intensity or crystallinity of the samples would be increased by rising the temperature of calcination [27]. However, some salt components including NaCl at the certain peaks of spent TiO₂ and POFA were detected due to low calcination temperature in Fig. 2. Various other studies have also indicated the similar peaks for salts at about 2θ of at 32.20° and 45.50° for spent TiO₂ photocatalysts. Moreover, the two more impurities for NaCl at 2θ of 40.77 and 46.20 was detected for ash samples [5, 28]. That could possibly be the reason that the surface area and pore size and volume was drastically decreased for the spent ash samples (see Table 1).

Interestingly, the hybrid samples of Ti:Ash (60:40 and 40:60) photocatalysts found the peaks for both crystalline silica at 2θ of 26.811° and anatase phase of TiO₂ at 2θ 25.475°. Fig. 2 clearly shows that peaks of NaCl for Ti:Ash 60:40 and 40:60, both share same peaks profile which is observed at 2θ of 32.1°, 36.90°, 45.80°, 54.26°, and 56.85° with a relatively better appearance for Ti:Ash 60:40 photocatalyst which indicating a good absorption capability comparing to Ti:Ash 40:60 photocatalyst. Furthermore, for both spent and fresh catalysts the peaks of SiO₂ were detected at 2θ of 21.33°, 26.92°, and 76.43°. It was expected that the silica content in POFA might enhance the catalyst in seawater pretreatment by improving the absorbance of the photocatalyst [29].

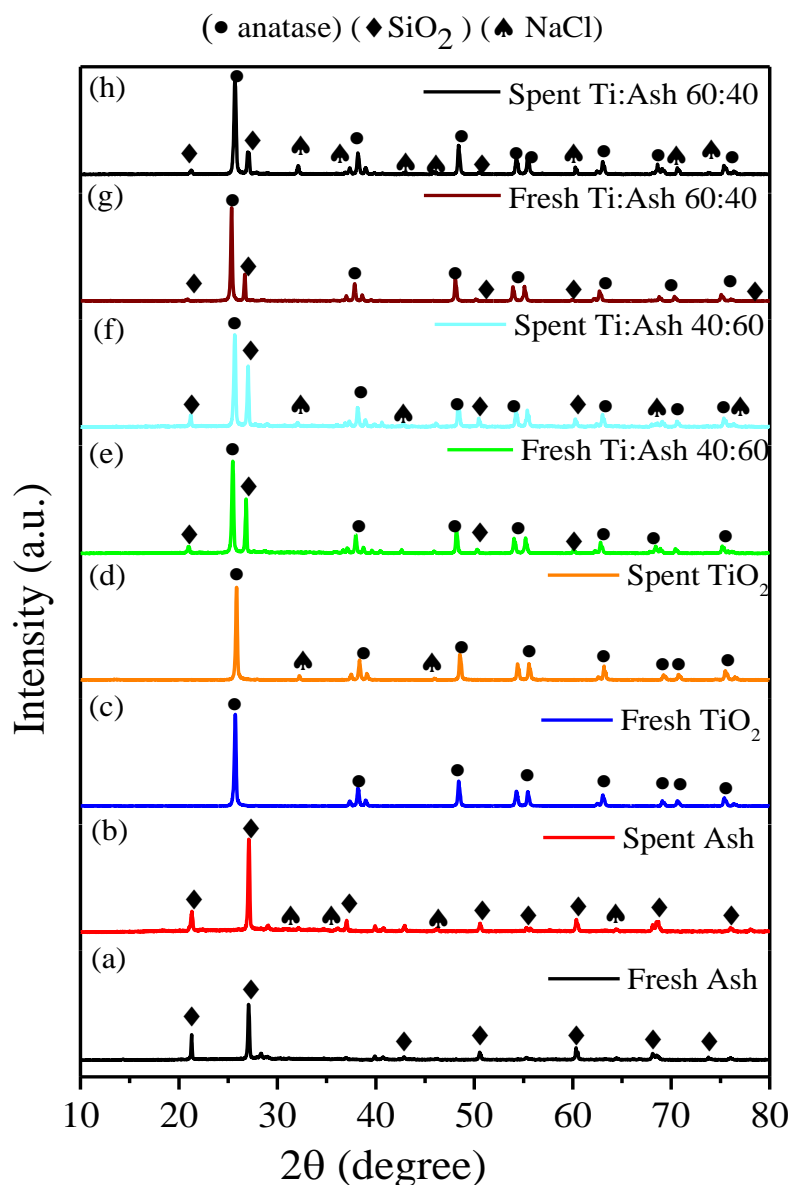


Figure 2: XRD patterns of fresh and spent photocatalysts, (a) fresh ash (b) spent ash (c) fresh TiO₂ (d) spent TiO₂ (e) fresh Ti: Ash 40:60 (f) spent Ti: Ash 40:60 (g) fresh Ti: Ash 60:40 (h) spent Ti: Ash 60:40.

B. Effect of TiO₂:Ash on artificial seawater (ASW) treatment

As shown in Fig. 3, different properties such as pH, conductivity, TDS, COD, and Turbidity were tested for artificial water. Turbidity of 100% Ash-based was decreased by 51 % (from 4.3 NTU to 2.1 NTU) after the photocatalytic reaction. On the other hand, it was reduced by 47 % (4.3 NTU to 2.26 NTU) for 100% TiO₂ (Ti:Ash of 100:0) samples after photocatalytic reaction, while amount of turbidity was not changed. but after using the hybrid Ti:Ash 40:60. photocatalysts the artificial seawater turbidity was decreased by 49 % from 4.03 NTU to 2.06 NTU, besides it was reduced by 41 % (4.03 NTU to 2.36 NTU) for used Ti:Ash 60:40 photocatalyst. The reduced of the water turbidity causes by filtration process that was carried out to separate the catalysts from samples and might related to the degradation of Humic as shows in Fig. 3. In addition, the COD of Ti:Ash 100:0 was reduced from 775 mg L⁻¹ to 510 mg L⁻¹ and 34% reduction compared to Ti:Ash 0:100 which decline from 775 mg L⁻¹ to 550 mg L⁻¹ which was up to 2914 reduction. Whereas the seawater treated without a catalyst the value of COD went down by 7 % only from 750 mg L⁻¹ to 720 mg L⁻¹ as shown in Fig. 4(b). Other studies have also reported that TiO₂ can adsorb and degrading water contaminates by photoreaction [30].

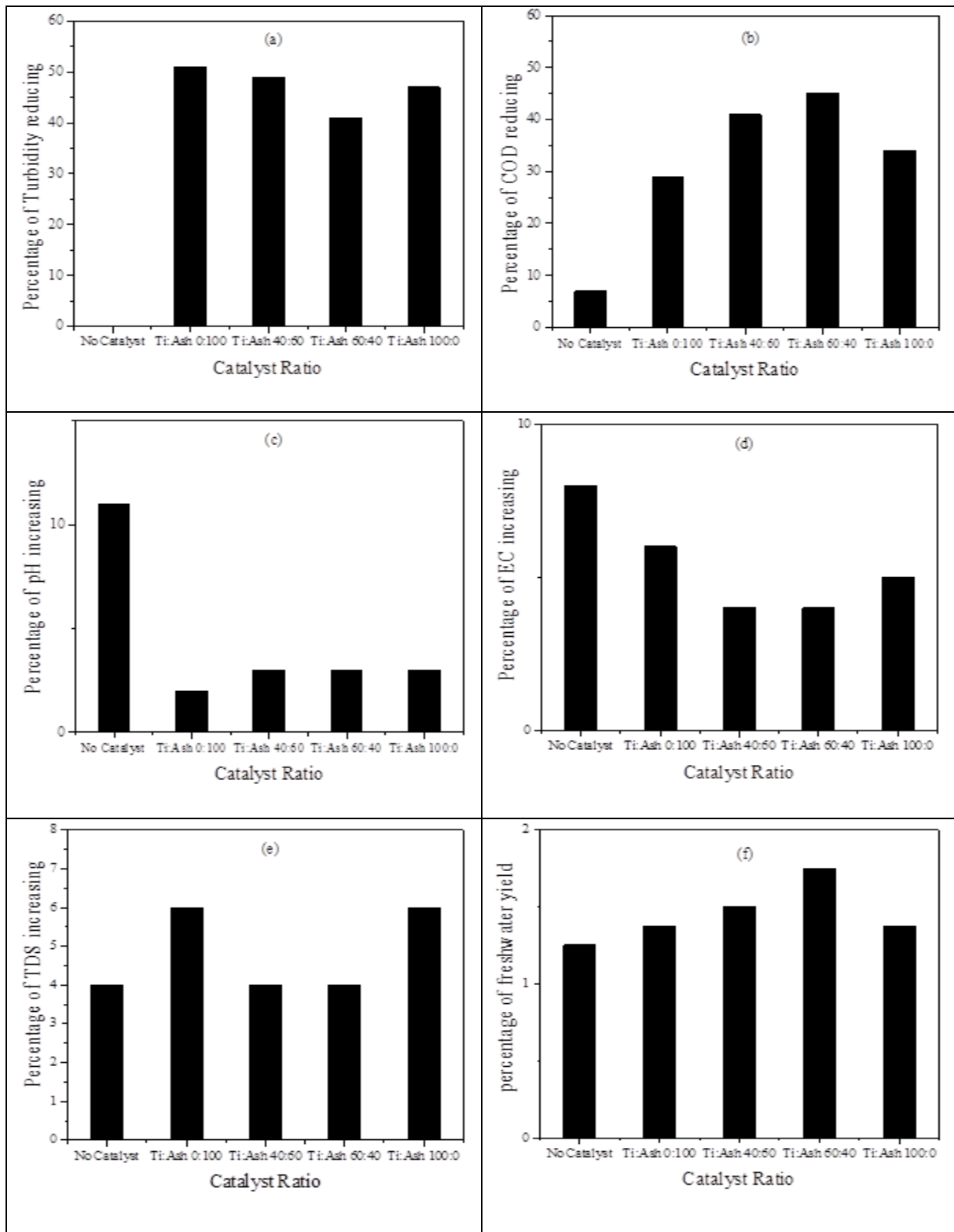


Figure 3: Analytical test of seawater were treated by all catalysts: (a) Turbidity (b) COD (c) PH (d) Conductivity (e) TDS (f) freshwater yield

There is a difference in the percentage of decline where it can be note that for Ti:Ash 60:40 the ratio was 41 % comparing to 49 % was for Ti:Ash 40:60 which might related to TiO_2 ratio in Ti:Ash 60:40 which is more than Ti:Ash 40:60. Furthermore, the COD of seawater reduced after treated by using Ti:Ash 40:60 decreased by up to 41 % from 775 mg L^{-1} to 460 mg L^{-1} . Whereas the seawater treated by Ti:Ash 60:40 which declined from 775 mg L^{-1} to 430 mg L^{-1} which was up to 45 % reduction as shown in the figure 4(a) and 4(b). The decline of the value of the chemical oxygen demand, indicating that the organic and inorganic matter in artificial seawater (represented in humic acid) can be reduced. Bekbolet and Ozkosemenn [31] investigated

that the photocatalytic degradation using humic acid as a model and observed that after 1 h in the presence of irradiation and by using 1.0 g L⁻¹ of TiO₂ (P25), 40 % TOC and 75 % of the color were removed. On the other hand, Eggins and coworkers [32] found the irradiated of TiO₂ (P25) by a mercury lamp and exhibited a very efficient reduction of humic acid concentration about 50% in 12 min. Olanders and Steenari [33] claimed that the biomass ash was rich with Ca, Si, Al, Ti, Fe, Na, Mg, K, P, and S which can enhance the adsorbent property to remove water contaminants.

The PH of artificial seawater increased by 2 % and 3 % after treated with bare TiO₂ and palm oil fiber ash respectively. While when treated without the percentage of pH increasing was 11 %. Whereas, the pH also increased from 6.90 to 7.11 by 3 % when Ti:Ash 40:60 was used. Besides, there was the almost same change in seawater pH when Ti:Ash 60:40 was used which by 3 % as showing in Fig. 3(c). From Fig. 3(d) the conductivity of ASW slightly increased from 42.76 mS cm⁻¹ to 45.23 mS cm⁻¹ and 45 mS cm⁻¹ by 5 % and 6 % when treated with Ti:Ash 100:0 and Ti:Ash 0:100, respectively. Meanwhile, the EC of the sample which was treated without catalyst also increased from 42.6 mS cm⁻¹ to 45.93 mS cm⁻¹ around 8 %. Fig. 3(d) indicates that the conductivity of seawater which treated with Ti:Ash 40:60 increased from 43.23 mS cm⁻¹ to 44.83 mS cm⁻¹. While the sample which was tested by Ti:Ash 60:40 also increased from 42.30 mS cm⁻¹ to 44 mS cm⁻¹ by the same percentage for both catalysts which signifies of up to 4%. Furthermore, Fig. 3 also revealed that the amount of total dissolved solids increases by 6% with the same value in seawater from 27.4 mg L⁻¹ to 29 mg L⁻¹ after treated with Ti:Ash 100:0 and Ti:Ash 0:100. While in absent the catalyst the TDS also increased from 27.3 mg L⁻¹ to 28.3 mg L⁻¹ by 4 % as shown in the Fig. 2f. Furthermore, Fig. 2(f) also revealed that the amount of total dissolved solids increased by 6 % with the same value in seawater from 27.4 mg L⁻¹ to 29 mg L⁻¹ after treated with Ti:Ash 100:0 and Ti:Ash 0:100. While in absent the catalyst the TDS also increased from 27.3 mg/L to 28.3 mg/L by 4 % as shown in the Fig. 3. Furthermore, the TDS of seawater increased slightly by the same percentage which is 4 %, from 27.3 g L⁻¹ to 28.26 g L⁻¹ and from 27 g L⁻¹ to 28.20 g L⁻¹ when Ti:Ash 40:60 and Ti:Ash 60:40 were used, respectively. The amount of increase does not significant because the TiO₂ and Ash also absorbing some amount of salts. Beside that the change in PH value it might be due to alkaline materials which found in oil palm fiber ash [34].

It clearly can be seen in Table 2 the amount of water distilled and yield rate for seawater which was treated without a catalyst, Ti:Ash 0:100, Ti:Ash 40:60, Ti:Ash 60:40, and Ti:Ash 0:100. From Table 2, the highest freshwater production rate was achieved at 14 ml by yield (1.75 %) rate when Ti:Ash 60:40 was used. whereas the lowest rate was 10 mL with a production rate of up to (1.25%) when the seawater treated without a catalyst. While Ti:Ash 40:60 produced 12 mL of fresh water with (1.50 %) yield rate. Also, both of bare TiO₂ and Ti:Ash 0:100 showed the same trend for yield rate which was (1.37 %) with 11 ml of distillate water as showing in figure 4f.

Table 2: Amount and Yield fresh water after testing

Catalyst type	Without Catalyst	TiO ₂ :Ash 0:100	TiO ₂ :Ash 40:60	TiO ₂ :Ash 60: 40	TiO ₂ :Ash 100: 0
Analytical test					
Amount of fresh water (Kg)	0.010	0.015	0.012	0.014	0.011
Volume of fresh water (mL)	10	11	12	14	11
Yield of fresh water (%)	1.25	1.37	1.50	1.75	1.37

Table 3 shows that the comparison between freshwater produced during photocatalytic pretreatment of seawater with National Water Quality Standards for Malaysia. It can be seen in Table 3 that the distillate water has a pH at 7.15, a conductivity of 75.89 µS/cm, a total dissolved solid 48.25 mg/l, a chemical oxygen demand of 5 mg/L and a turbidity of 0.29 NTU. In comparison to standard A of drinking water specification, the distillate water that produced via distillation complied with the standard specification.

Table 3: Analyzed data of produced distillate water

Catalyst type / Analytical test	Fresh water produced	National Water Quality Standards for Malaysia*
PH	7.15	6.5 – 8.5
Conductivity($\mu\text{S}/\text{cm}$)	75.89	< 1000
TDS (mg/L)	48.25	< 500
COD (mg/L)	5	< 10
Turbidity (NTU)	0.29	< 5

* National Water Quality Standards for Malaysia (Source: EQR2006)

4. CONCLUSIONS

In this paper, effect of mass ratio of titanium dioxide and oil palm fiber ash (TiO_2 : Ash) in hybrid photocatalyst to seawater pretreatment, showed that the activity of TiO_2 for seawater pretreatment was enhanced by hybrid with oil palm fiber ash (OPFA) with two different mass ratio which is Ti:Ash 40:60 and Ti:Ash 60:40. XRD pattern revealed that the hybrid of OPFA did not convert the crystalline phase of the TiO_2 besides improving the pore size, and pore volume while the surface area was almost same. Moreover, both catalysts are able to adsorb salt (NaCl). For chemical oxygen demand (COD) degradation test, bare TiO_2 , and Ash exhibited low activity under UV-light irradiation comparing to Ti:Ash 40:60 and Ti:Ash 60:40. Significant enhancement was observed when Ti:Ash 40:60 was used (45 % of COD degradation) compared to 41% of COD degradation for Ti:Ash 60:40. On the other hand, artificial seawater (ASW) gives results closely paralleling those with natural seawater (NSW) and can be used for catalyst evaluation and the simulation of NSW. The combination of TiO_2 and oil palm fiber ash improved the photocatalytic activity and adsorbent of salt.

ACKNOWLEDGMENT

This work was supported by Universiti Malaysia Pahang (UMP) [RDU1703242].

REFERENCES

- [1] M. A. Shannon, P. W. Bohn, M. Elimelech, J. G. Georgiadis, B. J. Marinas, A. M. Mayes, "Science and technology for water purification in the coming decades," *Nature*, vol. 452, p. 301, 2008.
- [2] D. P. Loucks, E. Van Beek, *Water resource systems planning and management: An introduction to methods, models, and applications*: Springer, 2017.
- [3] M. Elimelech, W. A. Phillip, "The future of seawater desalination: energy, technology, and the environment," *science*, vol. 333, pp. 712-717, 2011.
- [4] H. Yuan, "Bioelectrochemical Systems: Microbiology, Catalysts, Processes and Applications," Virginia Tech, 2017.
- [5] W. E. Kan, J. Roslan, R. Isha, "Effect of Calcination Temperature on Performance of Photocatalytic Reactor System for Seawater Pretreatment," *Bulletin of Chemical Reaction Engineering & Catalysis*, vol. 11, p. 230, 2016.
- [6] M. Kamboj, A. Dhir, "Studies On The Degradation Of Industrial Wastewater Using Heterogeneous Photocatalysis," 2009.
- [7] S. Sarina, E. R. Waclawik, H. Zhu, "Photocatalysis on supported gold and silver nanoparticles under ultraviolet and visible light irradiation," *Green Chemistry*, vol. 15, pp. 1814-1833, 2013.
- [8] R. A. A-. Rasheed, "Water treatment by heterogeneous photocatalysis an overview," in 4th SWCC acquired Experience Symposium held in Jeddah, 2005, pp. 1-14.
- [9] Z. Wu, C. Gong, J. Yu, L. Sun, W. Xiao, C. Lin, "Enhanced visible light photoelectrocatalytic activity over $\text{Cu}_x\text{Zn}_{1-x}\text{In}_2\text{S}_4/\text{TiO}_2$ nanotube array hetero-structures," *Journal of Materials Chemistry A*, vol. 5, pp. 1292-1299, 2017.
- [10] B. Ohtani, O. Prieto-Mahaney, D. Li, R. Abe, "What is Degussa (Evonik) P25? Crystalline composition analysis, reconstruction from isolated pure particles and photocatalytic activity test," *Journal of Photochemistry and Photobiology A: Chemistry*, vol. 216, pp. 179-182, 2010.
- [11] A. O. Ibhaddon, P. Fitzpatrick, "Heterogeneous photocatalysis: recent advances and applications," *Catalysts*, vol. 3, pp. 189-218, 2013.

- [12] M.-h. Wu, L. Li, N. Liu, D.-j. Wang, Y.-c. Xue, L. Tang, "Molybdenum disulfide (MoS₂) as a co-catalyst for photocatalytic degradation of organic contaminants: A review," *Process Safety and Environmental Protection*, 2018.
- [13] B. Guo, H. Shen, K. Shu, Y. Zeng, W. Ning, "The study of the relationship between pore structure and photocatalysis of mesoporous TiO₂," *Journal of chemical sciences*, vol. 121, pp. 317-321, 2009.
- [14] K. H. Ng, C. H. Lee, M. R. Khan, C. K. Cheng, "Photocatalytic degradation of recalcitrant POME waste by using silver doped titania: Photokinetics and scavenging studies," *Chemical Engineering Journal*, vol. 286, pp. 282-290, 2016.
- [15] W. Tangchirapat, T. Saeting, C. Jaturapitakkul, K. Kiattikomol, A. Siripanichgorn, "Use of waste ash from palm oil industry in concrete," *Waste Management*, vol. 27, pp. 81-88, 2007.
- [16] A. Demirbas, "Potential applications of renewable energy sources, biomass combustion problems in boiler power systems and combustion related environmental issues," *Progress in energy and combustion science*, vol. 31, pp. 171-192, 2005.
- [17] S. Yaman, "Pyrolysis of biomass to produce fuels and chemical feedstocks," *Energy conversion and management*, vol. 45, pp. 651-671, 2004.
- [18] T. Ahmad, M. Danish, M. Rafatullah, A. Ghazali, O. Sulaiman, R. Hashim, et al., "The use of date palm as a potential adsorbent for wastewater treatment: a review," *Environmental Science and Pollution Research*, vol. 19, pp. 1464-1484, 2012.
- [19] O. Sacco, V. Vaiano, M. Matarangolo, "ZnO supported on zeolite pellets as efficient catalytic system for the removal of caffeine by adsorption and photocatalysis," *Separation and Purification Technology*, vol. 193, pp. 303-310, 2018.
- [20] D. S. Kim, S. J. Han, S.-Y. Kwak, "Synthesis and photocatalytic activity of mesoporous TiO₂ with the surface area, crystallite size, and pore size," *Journal of Colloid and Interface Science*, vol. 316, pp. 85-91, 2007.
- [21] J. Nichols, A. Smith, "Naive and primed pluripotent states," *Cell stem cell*, vol. 4, pp. 487-492, 2009.
- [22] T. Katou, B. Lee, D. Lu, J. N. Kondo, M. Hara, K. Domen, "Crystallization of an ordered mesoporous Nb-Ta oxide," *Angewandte Chemie International Edition*, vol. 42, pp. 2382-2385, 2003.
- [23] D. Grosso, C. Boissière, B. Smarsly, T. Brezesinski, N. Pinna, P. A. Albouy, et al., "Periodically ordered nanoscale islands and mesoporous films composed of nanocrystalline multimetallic oxides," *Nature materials*, vol. 3, p. 787, 2004.
- [24] Q. Sun, X. Hu, S. Zheng, Z. Sun, S. Liu, H. Li, "Influence of calcination temperature on the structural, adsorption and photocatalytic properties of TiO₂ nanoparticles supported on natural zeolite," *Powder Technology*, vol. 274, pp. 88-97, 2015.
- [25] J. F. Porter, Y.-G. Li, C. K. Chan, "The effect of calcination on the microstructural characteristics and photoreactivity of Degussa P-25 TiO₂," *Journal of materials science*, vol. 34, pp. 1523-1531, 1999.
- [26] E. F. Heald, C. W. Weiss, "Kinetics and mechanism of anatase/rutile transformation, as catalyzed by ferric oxide and reducing conditions," *American Mineralogist*, vol. 57, pp. 10-&, 1972.
- [27] G. P. Maniam, N. Hindryawati, M. Yusoff, "Rice Husk Silica Supported Oil Palm Fruit Ash as a Catalyst in the Transesterification of Waste Frying Oil," *Journal of Engineering and Technology (JET)*, vol. 6, pp. 1-12, 2015.
- [28] Ş. Yalçın, I. Mutlu, "Structural characterization of some table salt samples by XRD, ICP, FTIR and XRF techniques," *Acta Physica Polonica-Series A General Physics*, vol. 121, p. 50, 2012.
- [29] H. Jamo, M. Z. Noh, Z. A. Ahmad, "Structural analysis and surface morphology of a treated palm oil fuel ash," 2013.
- [30] H. Sun, S. Liu, S. Liu, S. Wang, "A comparative study of reduced graphene oxide modified TiO₂, ZnO and Ta₂O₅ in visible light photocatalytic/photochemical oxidation of methylene blue," *Applied Catalysis B: Environmental*, vol. 146, pp. 162-168, 2014.
- [31] M. Bekbölet, G. Özköşemen, "A preliminary investigation on the photocatalytic degradation of a model humic acid," *Water Science and Technology*, vol. 33, pp. 189-194, 1996.
- [32] B. R. Eggins, F. L. Palmer, J. A. Byrne, "Photocatalytic treatment of humic substances in drinking water," *Water research*, vol. 31, pp. 1223-1226, 1997.
- [33] B. Olanders, B.-M. Steenari, "Characterization of ashes from wood and straw," *Biomass and Bioenergy*, vol. 8, pp. 105-115, 1995.
- [34] I. Udoetok, "Characterization of ash made from oil palm empty fruit bunches (oefb)," *International Journal of Environmental Sciences*, vol. 3, pp. 518-524, 2012.
- [35] DOE, "Malaysia environmental quality report 2014," Ministry of Natural Resources and Environment, Chapter 3: River Water Quality, pp. 47-67, Accessed 20 Apr 2018.